applied sciences

MDPI

Article

A Mathematical Model for the Initial Interaction Stage Between a Radar System and a Target Using GERT Network

Serhii Semenov [1], Magdalena Krupska-Klimczak [1,*], Patryk Mieczkowski [1], Yevhen Tarasenko [2], Vitalii Voronets [2], Oleksandr Voronets [2], Vitalii Breslavets [2] and Viacheslav Davydov [3]

[1] Cyber Security Department, University of the National Education Commission, ul. Podchorążych 2, 30-084 Kraków, Poland; serhii.semenov@uken.krakow.pl (S.S.); patryk.mieczkowski@uken.krakow.pl (P.M.)
[2] Department of Information Systems, National Technical University "Kharkiv Polytechnic Institute", Kyrpychova Str., 2, 61002 Kharkiv, Ukraine; yevhen.tarasenko@cit.khpi.edu.ua (Y.T.); vitalii.voronets@khpi.edu.ua (V.V.); oleksandr.voronets@infiz.khpi.edu.ua (O.V.); vitalii.breslavets@khpi.edu.ua (V.B.)
[3] Department of Information Technology and Cyber Security, Science Entrepreneurship Technology University, M. Shpaka St., 3, 03113 Kiyv, Ukraine; vyacheslav.v.davydov@gmail.com
* Correspondence: magdalena.krupska-klimczak@uken.krakow.pl

Abstract: The article presents a mathematical model of radar systems operating under jamming conditions. The relevance of the study is highlighted by two main factors: the need to enhance the accuracy of radar systems and the requirement to incorporate new jamming factors into models, which raises challenges in maintaining the reliability of mathematical formalizations. Various modeling approaches, including Markov models, deep learning, and probabilistic filters, are analyzed. These methods enable radar systems to adapt to changing conditions and improve target detection, which are crucial for their effective operation under uncertainty. The article emphasizes the importance of integrating different techniques to develop algorithms capable of functioning in complex jamming environments. A key aspect of the model is its consideration of time delays and probabilistic characteristics, which help to formalize and optimize the system's performance in various jamming scenarios. The model is based on the Graphical Evaluation and Review Technique (GERT) network, offering in-depth analysis and adaptation of radar systems to changing conditions. This approach is a critical component for enhancing the resilience of radar systems in complex and uncertain operational environments.

Keywords: radar systems; mathematical modeling; target tracking; GERT networks

Academic Editor: Atsushi Mase

Received: 20 December 2024
Revised: 17 January 2025
Accepted: 20 January 2025
Published: 23 January 2025

Citation: Semenov, S.; Krupska-Klimczak, M.; Mieczkowski, P.; Tarasenko, Y.; Voronets, V.; Voronets, O.; Breslavets, V.; Davydov, V. A Mathematical Model for the Initial Interaction Stage Between a Radar System and a Target Using GERT Network. *Appl. Sci.* **2025**, *15*, 1123. https://doi.org/10.3390/app15031123

1. Introduction

1.1. Motivation

Radar systems form an integral part of modern infrastructure, with diverse applications ranging from defense to civilian use. They play a key role in ensuring safety and effectiveness in challenging conditions such as nighttime operations, poor visibility, and adverse weather. As technology advances and the number of unmanned systems and robotic platforms increases, the demands for greater accuracy, reliability, and data security in radar operations are also rising. These factors highlight the importance of ongoing research in this field.

One of the most significant challenges modern radar systems face is the high level of interference, which can stem from both natural sources (e.g., atmospheric phenomena and meteorological conditions) and artificial sources (e.g., electronic warfare and electromagnetic interference). Such interference can greatly reduce the effectiveness of target

detection and tracking, increase the likelihood of false alarms, and affect the accuracy of radar measurements.

Addressing the impact of interference is critical for the development and operation of radar systems. Inadequate interference management can lead to severe consequences such as data loss, system malfunctions, and compromised security compliance.

Improving radar data processing technologies requires advancements not only in hardware and signal processing algorithms but also in developing effective mathematical models to predict and optimize radar performance in various conditions, including those with interference. Mathematical formalization of radar data processing will allow consideration of multiple interference-related aspects and characteristics.

Modeling enables the analysis of how different systems and environmental parameters affect key radar performance indicators. It allows for the consideration of complex interference effects, system parameter optimization, and simulations of radar operation in various scenarios (e.g., combat conditions, severe weather, long-distance operations). This adaptability helps configure models for specific radar tasks and operating conditions.

1.2. State-of-the-Art

Given the evolving challenges and diverse methodologies in radar system modeling, this section reviews key approaches and highlights gaps addressed in this study.

The literature review should begin with the monograph [1], which serves as a foundational scientific work emphasizing the importance of radar system operation and the complexity of this process in the presence of interference. This work is a comprehensive study of a specific topic, aimed at providing in-depth knowledge and analyses. It covers various aspects, including definitions, historical context, current trends, challenges, and future implications. At the same time, the author of the monograph highlights the need for further research and practical actions to improve the efficiency of radar system operations.

A review of the literature reveals a wide variety of approaches to mathematical modeling and current challenges in formalizing radar system data processing.

Thus, in the article [2], the importance of using radar systems in areas such as air traffic control, automotive safety, and environmental monitoring is noted. The relevance of improving the efficiency of radar systems operation in the presence of interference is emphasized. The article highlights the variety of approaches to solving this problem, including innovative ones, such as “Bioinspired Design”.

Several studies present simulation results based on various formalizing concepts. For example, in article [3], the problem of detecting subspace random signals against correlated non-Gaussian noise is considered, using different levels of knowledge about the statistical characteristics of both target signals and interference. The noise is modeled using a complex Gaussian distribution. Unfortunately, the authors do not provide a practical implementation algorithm for this development, which somewhat limits the applicability of the results presented in this article.

In [4], the authors present a mathematical formalization approach using an adaptive extended Kalman filter with strong tracking capabilities. They introduce adaptive damping elements to enhance filtering accuracy and reduce the divergence problems associated with strong tracking methods. While this improves the estimate quality during tracking, the model is sensitive to noise, and its effectiveness deteriorates in the presence of anomalous emissions. Additionally, the algorithm requires regular updates to adaptive damping factors, which increases computational costs and complexity.

In [5], the authors develop a Multiple-Model Gaussian Mixture Probability Hypothesis Density (MMGM-PHD) filter to improve the tracking of multiple objects in scenarios with predetermined trajectories, particularly in land, sea, and air transport control. By

incorporating hybrid models, the authors account for target maneuverability, which is difficult to address using homogeneous models. However, this method may be less effective in scenarios where targets behave unpredictably or deviate from predetermined paths.

The authors of article [6] use a Markov model and a universal finite automaton, which allow for expanding the options for assessing target detection capabilities. Among the strengths of the work are its well-structured presentation and discussion of existing challenges, as well as an innovative approach to performance evaluation using different levels of abstraction. However, the study does not provide sufficient data to fully assess the feasibility of the proposed methodology in various operational scenarios. This could be an area for future research focused on further optimizing methods in the field of radar system operation.

In [7], the authors explore the use of artificial intelligence in radar signal estimation, proposing a denoising autoencoder (DAE) and deep neural network (DNN) scheme. Simulations conducted at various signal-to-noise ratios demonstrate the DAE's ability to overcome limitations in existing techniques and open up new possibilities for high-resolution direction-of-arrival (DoA) estimation in complex environments. However, training deep neural networks requires large amounts of data, which can be challenging in resource-limited or data-scarce settings.

A conference report in [8] discusses the development of a method for feature extraction in unmanned aerial vehicle (UAV) motion modeling using a variational autoencoder, further exploring artificial intelligence applications in air target tracking under external influences.

In [9], the authors present another effective approach to mathematical formalization, focusing on managing telecommunication network parameters under uncertainty caused by both natural and anthropogenic factors. The study suggests that the principles used in telecommunication networks can be adapted for radar systems, offering insights into assessing radar timing, target detection accuracy, and resistance to interference.

Several articles, including [10], address the issue of adaptive algorithms for generating and tracking target trajectories at different stratification levels. In [10], the authors focus on tracking maneuvering air targets, proposing an adaptive tracking algorithm that switches between uniform and maneuvering motion models. Although this approach offers a solution to the challenges posed by fuzzy models and target dynamics, the lack of comparative studies with similar algorithms limits the ability to evaluate its reliability.

In [11], the authors propose an improved algorithm for multidimensional target tracking in aircraft radar systems using Doppler technology. The algorithm, based on a Bayesian approach and random finite set (RFS) theory, effectively suppresses interference in complex conditions, avoiding traditional computational complexities.

Reducing computational complexity while maintaining accuracy and reliability is a common goal in mathematical formalization research. In [12], fuzzy GERT modeling methods are analyzed to increase the accuracy of process formalization in software vulnerability studies under uncertain conditions. This suggests the potential for applying similar approaches in radar system modeling.

Further evidence of this potential is found in [13,14], where the authors explore GERT network modeling to enhance the efficiency of mathematical formalization under uncertainty.

In [15], the development of a pulsed Doppler radar system model using MATLAB 9.5/Simulink is presented, offering a comprehensive example of simulation modeling. The study confirms the relevance of the chosen research direction.

In [16], the theoretical basis of radar operation, including range and angle tracking mechanisms, is presented. The study also explores radar jamming technologies such as noise and deception jamming and develops an electronic attack simulator. While simulation

modeling proves effective at certain research stages, simulating electronic attack scenarios can be complex and resource intensive.

Finally, in [17,18], the authors analyze various factors affecting radar performance, including uncertainty in radar positions and interference screening. Despite providing valuable insights, these studies often overlook the importance of measuring the interaction time between the radar and tracked object as an indicator of radar efficiency.

In comparison to existing model-based schemes, such as the approach by [19], which focuses on interference suppression strategies using Markov Chain Monte Carlo (MCMC) in low- and medium-interference environments, our proposed model emphasizes scenarios with high dynamic jamming. The use of GERT networks provides macro-level probabilistic analysis, while the Kalman filter enhances micro-level parameter refinement.

Similarly, the model developed by [20], which leverages deep learning for trajectory optimization in radar systems, differs from our approach by focusing on machine learning-based methods. In contrast, our work combines probabilistic models and deterministic algorithms, ensuring adaptability and robustness across a wide range of interference conditions. These distinctions highlight the unique contributions of our study in advancing radar system performance under jamming conditions.

Overall, the literature analysis underscores the relevance of mathematical modeling of radar operation under interference conditions. To further this research, a generalized algorithm for tracking target trajectories will be developed to identify a system of radar noise immunity indicators.

1.3. Objectives and Contributions

The aim of this research is to develop a mathematical model of the radar system's operational process and to analytically evaluate its probabilistic and temporal characteristics, specifically in the context of formalizing the algorithm for tracking an airborne target's trajectory under external influences.

The main objectives are as follows:

- To establish a formalized algorithm for aerial target trajectory tracking;
- To develop a mathematical model of radar system performance under external interference conditions;
- To analyze the probabilistic and temporal characteristics of the interaction channel between the radar and an object emitting active interference.

To achieve the stated goal, the following tasks must be completed:

- Investigate the target tracking algorithm;
- Develop a mathematical model of radar system operation under interference conditions;
- Study the probabilistic and temporal characteristics of the interaction channel between the radar system and an object generating active interference.

2. Algorithm for Tracking Target Trajectories

The radar system operation process can be divided into two main stages: radar signal processing and radar data processing. These stages are closely related, but they have different functionality, purpose, and methods used. This division helps to better understand the functionality of the systems and their modeling.

The first stage of radar signal processing (radar signal processing stage) analyses the received echo signal to extract useful information. The main processes include the following:

- Signal pre-filtering. Used to suppress noise and interference occurring in the radar channel.

- CFAR (Constant False Alarm Rate). Adaptive false alarm control algorithms that highlight potential targets against a background of interference.
- Target Detection. Using corrected thresholds after CFAR, target coordinates, amplitudes and other characteristics are extracted. These processes are part of primary processing, where radar signals are analyzed to extract target-related data during a single radar scan.

The next stage is the data processing stage, which focuses on using the detected information to analyze the trajectories and behavior of targets. The key tasks in this stage are the following:

- Trajectory initialization. Combining multiple observations to form a track.
- Updating and maintaining the tracks. Using Kalman filters or other methods to refine target position based on new data.
- Motion prediction. Extrapolation of target position into the future based on mathematical models.

This stage is referred to as secondary processing, where multiple radar scans are analyzed to determine continuous target trajectories. These processing stages are tightly integrated into the overall algorithm for tracking target trajectories, as shown in Figure 1.

According to [21], the number of pulses transmitted by the radar to the target is determined by the antenna's rotation speed and the repetition rate of the probing pulses. For each range cell, a decision is made regarding the presence or absence of a target during each probing period. When a target is detected, a message is generated containing information such as the target's coordinates and other relevant data. This stage is referred to as "primary processing", as it involves collecting data from a single radar during one scan.

Following this, the process of determining the target's trajectory and locking onto it for tracking begins. At this stage, data from multiple radar scans are processed to identify and correlate observations related to the same target, forming a continuous trajectory—a single data set for each target. This is referred to as "secondary processing" of radar information. The block diagram of the algorithm for tracking a target's trajectory using data from one radar is shown in Figure 1.

Figure 1 illustrates the initial stage of the target detection process. A radar target typically generates several signals above the detection threshold across adjacent cells. These signals, along with their amplitudes, are used for interpolation to achieve more precise measurements. The following methods are employed to perform this task:

- Sliding window method (interpolation);
- Center of mass correlation (weighted averaging);
- Comparison with a database using ray shape (angular coordinate), impulse response (range), and Doppler filter shape (Doppler velocity).

The next phase of target trajectory tracking involves adaptive stabilization of the false alarm rate. The radar cross-section (RCS) distribution of air targets overlaps with the distribution of interference from scattering surfaces, increasing the number of false alarms as interference signals exceed the average detection threshold. To address this, an adaptive detection threshold is formed to stabilize the false alarm rate.

Once a target is detected, its trajectory is identified according to a specific algorithm. The trajectory is confirmed after the target is detected in three or more consecutive radar scans. This is called the "trajectory detection criterion", which is selected to avoid creating false trajectories. The detected marks are evaluated against the target motion hypothesis and the speed range for which the radar is designed. At this stage, the use of radar noise immunity indicators is critical. These include probabilistic, temporal, and spatial metrics under various interference conditions.

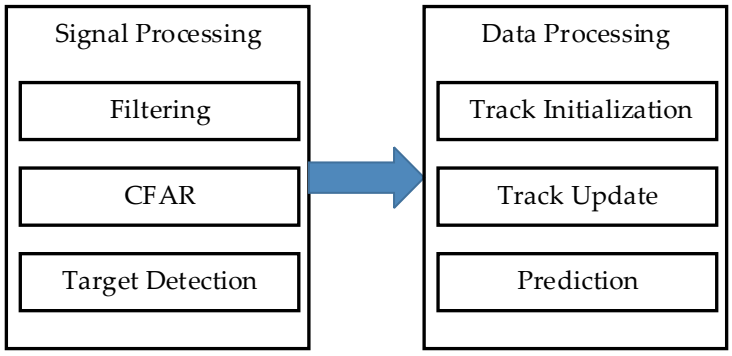

Figure 1. Block diagram of the algorithm for tracking a target's trajectory using data from a single radar.

The next step involves smoothing and extrapolating the trajectory. Based on previous target marks and the current scan, a smoothed estimate of the target's current position and velocity is generated. This estimate is then used to extrapolate the target's position for the next scan. An α-β filter (Kalman filter) is applied for extrapolation, considering jamming resistance metrics, such as accuracy in determining target coordinates and tracking stability under varying jamming conditions.

The final stages of the algorithm include trajectory tracking and updating. Trajectory data are stored in trajectory files. The main file contains information on all tracked trajectories, including measured coordinates, Doppler frequency, signal amplitude, timestamps, smoothed coordinates and velocities, extrapolated values for the next survey. When a target mark is associated with an existing trajectory, the trajectory is updated. During this stage, temporal noise immunity metrics are analyzed to optimize the target acquisition and trajectory update times.

If a target mark from the current survey cannot be associated with a tracked trajectory, a tracking strobe with expanded dimensions is created for the next survey. If target marks are absent in multiple surveys, the trajectory is reset. The criteria for resetting a trajectory may differ depending on the radar system. Spatial noise immunity indicators, such as tracking stability in varying noise environments, are also considered when resetting a trajectory.

The analysis of the algorithm indicates its relevance to studying radar noise immunity metrics, which encompass probabilistic, temporal, and spatial indicators. Prioritizing a specific set of indicators allows researchers to focus on certain areas of mathematical modeling and assess the effectiveness of the selected approach.

References [2,17,18,22] reveal a broad range of characteristics used in the mathematical formalization of radar system operations.

1. Probabilistic indicators:
   - probability of target detection;
   - probability of false alarm;
   - probability of correct classification;
   - probability of failure;
   - probability of failure to search for an object within given time;
   - probability of failure of capture the object within given time;
   - probability of failure to track an object within a given time;
   - probability of failure to transfer an object to the control and execution system within a given time.
2. Time indicators:
   - mean time between failures;
   - mean time to restore;

- system response time;
- data processing delay time;
- timeframes for failure in searching, capturing, tracking, and transfer with a certain probability.

3. Spatial indicators:
   - detection zone;
   - accuracy of coordinate determination;
   - resolution;
   - insensitivity zone;
   - spatial zones and radar suppression ranges.

Several indicators pertain to the radar's performance during key operations such as object search, capture, tracking, and transfer to the control and execution system. Key metrics include the following:

- $P_{search\_failure}(t)$—the failure probability of the object's searching over time;
- $P_{capture\_failure}(t)$—the failure probability of the object's capturing over time;
- $P_{tracking\_failure}(t)$—the failure probability of the object's tracking over specified time;
- $P_{transfer\_failure}(t)$—the failure probability of the object's transferring for servicing to the control and execution system over time;
- $t_{search\_failure}$—the search failure time;
- $t_{capture\_failure}$—the capture failure time;
- $t_{tracking\_failure}$—the tracking failure time;
- $t_{transfer\_failure}$—the transfer failure time to the control and execution system;
- The spatial zones in which the failure of operations $Z_{failure}$ is ensured;
- The spatial zones and radar suppression ranges where the failure of the problems' solution for search, capture, tracking, and transfer of an object for servicing $Z_{failure\_search}$, $Z_{failure\_capture}$, $Z_{failure\_resist}$, and $Z_{failure\_forward}$ is ensured with specified probability and time parameters.

These indicators can be used in the mathematical formalization process as components of a general indicator, such as radar interaction time with a tracked object. Ultimately, these metrics help in analyzing the efficiency of radar suppression under various interference conditions during the initial stages of mission execution.

Having established the operational framework, the next section delves into the mathematical foundation underpinning radar performance under interference conditions.

3. Mathematical Model of Radar Operation Under Interference Conditions

To develop a mathematical model for radar operation under jamming conditions, the GERT network modeling approach was selected. GERT (Graphical Evaluation and Review Technique) network is a probabilistic modeling tool used to analyze systems with complex dependencies. Unlike traditional network methods, GERT allows for probabilistic transitions and time delays. This makes it particularly valuable for studying processes with uncertainty, such as radar operation under interference conditions [12–14]. Several key advantages support the choice of this modeling technology:

1. Comprehensive representation of complex processes. During radar operation under jamming conditions, it is essential to account for all possible factors such as search, acquisition, tracking, and target transmission. Each of these stages can be affected by various failures or delays due to jamming. The GERT network allows for the visualization and formalization of these complex processes, incorporating probabilistic dependencies and time characteristics.

2. Analysis of various jamming scenarios. The GERT network enables the visualization and analysis of different jamming scenarios, including their occurrence probabilities and jamming intensities.
3. Time delays and their impact on system performance. GERT modeling accounts for the time characteristics of processes, allowing for the formalization of delays caused by jamming. This is particularly important for understanding how delays at different stages (search, acquisition, tracking) impact overall radar performance. Such insights are vital for optimizing system timing parameters.
4. Identification and analysis of critical paths. Under jamming conditions, it is crucial to identify critical paths where significant delays or disruptions might occur. The GERT network helps pinpoint and analyze these paths, aiding in the development of strategies to minimize or eliminate operational delays, ensuring better planning and protection at the design stage.
5. Visualization of processes and results. The GERT network provides a graphical representation of processes, making it easier to understand the radar's structure and behavior in jamming conditions. This enhances communication and analysis during the design and operational phases.

In summary, using the GERT network modeling approach for developing a radar operation model under jamming conditions offers a comprehensive way to incorporate probabilistic and time characteristics and to analyze jamming scenarios. These benefits highlight the potential of GERT modeling in addressing radar operation under challenging jamming environments.

Incorporating new jamming factors into mathematical models of radar systems represents a relevant and complex challenge that requires balancing increased model complexity with the need to maintain its reliability and computational efficiency. Jamming factors can include both natural sources of interference, such as atmospheric noise, and artificial ones, such as coordinated radar attacks and deceptive jamming techniques.

The proposed model addresses this challenge using several approaches. Firstly, each type of jamming is modeled using probabilistic distributions that reflect its temporal and spatial properties. For instance, noise jamming is represented by Gaussian distributions, while deceptive jamming may require the application of non-Gaussian or multimodal distributions. Such flexibility in modeling distributions is achieved through the use of GERT (Graphical Evaluation and Review Technique) modeling technology.

Secondly, a multi-layered modeling approach is applied, where the effects of interference are divided into distinct levels, such as noise, signal distortion, and false target generation. This allows the impact of each factor to be isolated and adjusted independently, without disrupting the overall system.

Moreover, the reliability of the model is assessed through iterative simulations in which the intensity and type of jamming are varied. Metrics such as the probability of detection, false alarm rate, and mean time to track loss are used to evaluate and optimize the model's performance.

The interaction between a radar and an object emitting active jamming can be represented through a GERT network with a discrete set of states and time intervals. The number of states in the network is determined by the decision-making algorithms used within the radar system:

$$\frac{k}{x} + \frac{x}{n} - h, \tag{1}$$

where k/x is establishing the object's trajectory criterion;

x/n is object trajectory detection confirmation criterion;

h object tracking reset criterion.

Equation (1) formalizes the criteria governing object trajectory detection, confirmation, and reset in a probabilistic GERT network framework.

The model time increment, dt, is determined based on the radar's time characteristics. Specifically, the time interval, dt, can be set equal to the period during which the radar interacts with the object.

Figure 2 presents a generalized GERT network that illustrates the radar's operation during its initial interaction with the tracked object, following an arbitrary algorithm described by the expression (1).

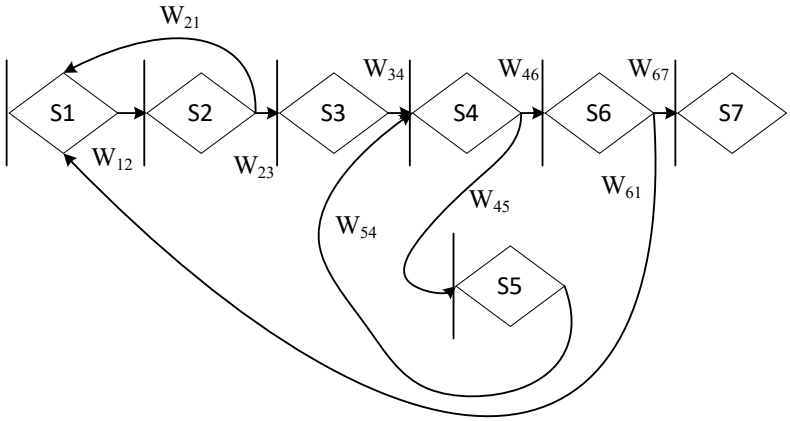

Figure 2. Generalized GERT network of radar operation in interaction with the tracking object at the initial stage.

In Figure 2 the transitions, nodes, and connections are defined as follows:

- Transition (1–2): Represents the process of detecting an echo signal from the tracked object;
- Transition (2–3): Records the event of forming a sufficient set of echo signals to establish a trajectory;
- Transition (2–1): Indicates the failure of the radar to use the set of echo signals to establish a trajectory;
- Connection (3–4): Formalizes the process of establishing the trajectory of the tracked object;
- Transition (4–6): Illustrates the final detection of the trajectory of the tracked object;
- Connection (4–5): Formalizes the radar's failure to complete the target task of final detection of the trajectory;
- Transition (5–4): Shows a return to the process of establishing the trajectory of the tracked object;
- Transition (6–7): Describes the ongoing tracking of the object;
- Transition (6–1): Formalizes the radar's failure in tracking the object;
- Nodes S1 and S7: Represent the "initial state of the system" and the "state characterizing successful tracking of the object", respectively;
- Nodes S2 to S6: Record the states of "forming a sufficient set of echo signals to establish a trajectory", "establishing a trajectory of the tracked object", "failure to establish a trajectory", "final detection of the trajectory", and the "tracking of the object".

When considering the possibility of transferring the tracked object for servicing to the monitoring and execution system, it is important to recognize that the time during which tracking may fail is limited by the radar's preparation time for the initial data on the tracked object. A key feature of this GERT network is that the tracking process, before the object's transfer for servicing, can be represented as a sequence of intermediate states corresponding to events where tracking does not fail during a specified time interval dt.

This must be considered in the mathematical description of transition (5–6). Reaching the final state of the chain, which corresponds to no failures in tracking during the specified time, indicates the successful transfer of the tracked object for servicing to the monitoring and execution system.

The use of the method of combining and describing fictitious states in GERT network modeling technology also allows for the analysis of the noise immunity of a radar system with a variable coverage period. The equivalent W-function of the radar functioning process in interaction with a tracked object at the initial stage can be expressed as:

$$W_E(\mathrm{s}) = \frac{W_{12}W_{23}W_{34}W_{46}W_{67} + W_{12}W_{23}W_{34}W_{45}W_{54}W_{46}W_{67}}{1 - W_{12}W_{21} - W_{12}W_{23}W_{34}W_{46}W_{34}W_{61}} \quad (2)$$

Let us derive an analytical relationship for calculating and studying the equivalent W-function of the radar operation process in its interaction with the tracking object during the initial stage.

To describe the characteristics of the branches of the GERT network in the radar operation process when interacting with the tracking object, we utilize the moment-generating function of the exponential distribution. This choice is justified by several key aspects:

- Analytical Convenience. The moment-generating function allows for straightforward manipulation of distributions when branches of the network are connected or processed in other ways. This is particularly beneficial for the exponential distribution, given the simplicity of its moment-generating function.
- Addition and Parallelism. In GERT networks, it is often necessary to analyze serial and parallel connections of branches. The moment-generating function for the exponential distribution provides a simple means to analyze such configurations.

Based on expression (2) and our research findings, we present the characteristics of the branches and the distribution parameters in Table 1.

Table 1. Characteristics of the functioning model branches process of the radar in interaction with the tracking object at the initial stage.

№	Branch	*W*-Function	Probability	Moment Generating Function
1	(1–2)	W_{12}	p_1	$\lambda_1/(\lambda_1 - s)$
2	(2–3)	W_{23}	p_2	$\lambda_2/(\lambda_2 - s)$
3	(2–1)	W_{21}	$1 - p_2 = q_1$	$\lambda_3/(\lambda_3 - s)$
4	(3–4)	W_{34}	p_3	$\lambda_4/(\lambda_4 - s)$
5	(4–5)	W_{45}	p_4	$\lambda_4/(\lambda_4 - s)$
6	(5–4)	W_{54}	p_4	$\lambda_5/(\lambda_5 - s)$
7	(4–6)	W_{46}	$1 - p_4 = q_2$	$\lambda_6/(\lambda_6 - s)$
8	(6–7)	W_{67}	p_5	$\lambda_7/(\lambda_7 - s)$
9	(6–1)	W_{61}	$1 - p_5 = q_3$	$\lambda_8/(\lambda_8 - s)$

Table 1 describes the key characteristics of the branches in a GERT network used to model the interaction process between the radar system and the tracking object at the initial stage. Each branch has a *W*-function, which accounts for both the transition probability and the timing characteristics through moment generation functions. In GERT networks, it is common to work with sequential and parallel branch connections, and for such operations, the exponential distribution provides particularly convenient formulas for calculating overall characteristics. This aspect is crucial for formalizing radar system operation processes, as the time periods before interaction with the object or task completion may vary, and the exponential distribution is ideal for describing them.

For the presented characteristics of the model branches, we will estimate the equivalent W-function of the radar operation process during its interaction with the tracking object at the initial stage. Let us describe the W-function for each branch as follows:

$$W_{ij} = p_k * \lambda_m, \tag{3}$$

where i, j are node numbers in the GERT network;

k is the probability index for the corresponding transition within the GERT network;

m is the generating function index of the corresponding transition moments within the GERT network.

λ is a key characteristic in the GERT model for describing transitions between different network states. It characterizes the rate of transitions or the interaction intensity of the network branch with the target under surveillance.

Since a GERT network represents a random graph network, λ in each transition reflects the probabilistic time required to move between the network nodes:

- λ_1 describes the detection rate of the radar system. The larger the value of λ_1, the faster the detection and transition to the next stage occur;
- λ_2 characterizes the intensity of interaction between nodes 2 and 3, related to signal processing or detection confirmation. This parameter depends on factors such as signal quality and noise level;
- λ_3 describes the probability of returning from node 2 to node 1. The value of λ_3 determines how often a return to the previous stage is required;
- λ_4 describes the transition intensity from node 3 to node 4, which may correspond to the initiation of target tracking. This time depends on radar parameters and target characteristics;
- λ_4 and λ_5 determine the transition intensity between the stages of track refinement and the need to return to previous stages for trajectory clarification;
- λ_6 characterizes the probability of a successful transition to the next stage of interaction, which is associated with completing the target tracking process and transferring control to the next node;
- λ_7 reflects the successful completion of the tracking process and the transition to the next stage, such as target confirmation;
- λ_8 is associated with returning to the beginning of the cycle, which may be caused by the need to revalidate data or detect new objects.

In this article, it is impossible to fully formalize and describe each of the presented parameters, λ_m. This will be the focus of further research and mathematical formalization.

Using expression (3) we obtain:

$$\mathrm{W_E}(s) = \frac{\frac{p_1 p_2 p_3 p_5 q_2 \lambda_1 \lambda_2 \lambda_4 \lambda_6 \lambda_7 \left((\lambda_5 - s)^2 + p_4^2 {\lambda_5}^2\right)}{(\lambda_1 - s)(\lambda_2 - s)(\lambda_4 - s)(\lambda_5 - s)^2(\lambda_6 - s)(\lambda_7 - s)}}{1 - \frac{\begin{pmatrix} p_1 q_1 \lambda_1 \lambda_3 (\lambda_2 - s)(\lambda_4 - s)(\lambda_6 - s)(\lambda_8 - s) \\ + p_1 p_2 p_3 q_2 q_3 \lambda_1 \lambda_2 \lambda_4 \lambda_6 \lambda_8 (\lambda_3 - s) \end{pmatrix}}{(\lambda_1 - s)(\lambda_2 - s)(\lambda_4 - s)(\lambda_6 - s)(\lambda_8 - s)}} \tag{4}$$

Through standard mathematical transformations, the following expression can be obtained for calculating the equivalent W-function of the radar operation process in interaction with the tracking object at the initial stage:

$$\mathrm{W_E}(s) = \frac{r\left(s^4 - ys^3 + us^2 - xs + c\right)}{(\lambda_7 - s)(s^7 + vs^6 + bs^5 + as^4 + ds^3 + fs^2 + gs + h)}, \tag{5}$$

where $r = p_1 p_2 p_3 p_5 q_2 \lambda_1 \lambda_2 \lambda_4 \lambda_6 \lambda_7$;

$y = \lambda_8 + \lambda_3$;
$u = \lambda_5^2 + 2\lambda_3\lambda_8 + 2\lambda_5\lambda_8 + 2\lambda_3\lambda_5 + p_4^2\lambda_5^2$;
$x = 2\lambda_5^2\lambda_8 + \lambda_3\lambda_5^2 + 2\lambda_3\lambda_5\lambda_8 + p_4^2\lambda_5^2\lambda_8 + p_4^2\lambda_5^2\lambda_3$;
$c = \lambda_5^2\lambda_8(\lambda_3 + p_4^2\lambda_3)$;
$v = -(\lambda_1 + \lambda_2 + \lambda_3 + \lambda_4 + \lambda_5 + \lambda_6 + \lambda_8)$;
$b = (\lambda_1\lambda_2 + \lambda_1\lambda_3 + \lambda_1\lambda_4 + \lambda_1\lambda_5 + \lambda_1\lambda_6 + \lambda_1\lambda_8 + \lambda_2\lambda_3 + \lambda_2\lambda_4 + \lambda_2\lambda_5 + \lambda_2\lambda_6 + \lambda_2\lambda_8 + \lambda_3\lambda_4 + \lambda_3\lambda_5 + \lambda_3\lambda_6 + \lambda_3\lambda_8 + \lambda_4\lambda_5 + \lambda_4\lambda_6 + \lambda_4\lambda_8 + \lambda_5\lambda_6 + \lambda_5\lambda_8 + \lambda_6\lambda_8 - p_1q_1\lambda_1\lambda_3(\lambda_2 + \lambda_4 + \lambda_6 + \lambda_8))$;
$a = (\lambda_1\lambda_2\lambda_3 + \lambda_1\lambda_2\lambda_4 + \lambda_1\lambda_2\lambda_5 + \lambda_1\lambda_2\lambda_6 + \lambda_1\lambda_2\lambda_8 + \lambda_1\lambda_3\lambda_4 + \lambda_1\lambda_3\lambda_5 + \lambda_1\lambda_3\lambda_6 + \lambda_1\lambda_3\lambda_8 + \lambda_1\lambda_4\lambda_5 + \lambda_1\lambda_4\lambda_6 + \lambda_1\lambda_4\lambda_8 + \lambda_1\lambda_5\lambda_6 + \lambda_1\lambda_5\lambda_8 + \lambda_1\lambda_6\lambda_8 + \lambda_2\lambda_3\lambda_4 + \lambda_2\lambda_3\lambda_5 + \lambda_2\lambda_3\lambda_6 + \lambda_2\lambda_3\lambda_8 + \lambda_2\lambda_4\lambda_5 + \lambda_2\lambda_4\lambda_6 + \lambda_2\lambda_4\lambda_8 + \lambda_2\lambda_5\lambda_6 + \lambda_2\lambda_5\lambda_8 + \lambda_2\lambda_6\lambda_8 + \lambda_3\lambda_4\lambda_5 + \lambda_3\lambda_4\lambda_6 + \lambda_3\lambda_4\lambda_8 + \lambda_3\lambda_5\lambda_6 + \lambda_3\lambda_5\lambda_8 + \lambda_3\lambda_6\lambda_8 + \lambda_4\lambda_5\lambda_6 + \lambda_4\lambda_5\lambda_8 + \lambda_4\lambda_6\lambda_8 + \lambda_5\lambda_6\lambda_8 - p_1\lambda_1q_1\lambda_3(\lambda_2\lambda_4 + \lambda_2\lambda_6 + \lambda_2\lambda_8 + \lambda_4\lambda_6 + \lambda_4\lambda_8 + \lambda_6\lambda_8) + p_1\lambda_1p_2\lambda_2p_3\lambda_4q_2\lambda_6q_3\lambda_8)$;
$d = -((\lambda_1\lambda_2\lambda_3\lambda_4 + \lambda_1\lambda_2\lambda_3\lambda_5 + \lambda_1\lambda_2\lambda_3\lambda_6 + \lambda_1\lambda_2\lambda_3\lambda_8 + \lambda_1\lambda_2\lambda_4\lambda_5 + \lambda_1\lambda_2\lambda_4\lambda_6 + \lambda_1\lambda_2\lambda_4\lambda_8 + \lambda_1\lambda_2\lambda_6\lambda_5 + \lambda_1\lambda_2\lambda_6\lambda_8 + \lambda_1\lambda_2\lambda_3\lambda_8\lambda_1\lambda_3\lambda_4 + \lambda_1\lambda_3\lambda_5 + \lambda_1\lambda_3\lambda_6 + \lambda_1\lambda_3\lambda_8 + \lambda_1\lambda_4\lambda_5 + \lambda_1\lambda_4\lambda_6 + \lambda_1\lambda_4\lambda_8 + \lambda_1\lambda_5\lambda_6 + \lambda_1\lambda_5\lambda_8 + \lambda_1\lambda_6\lambda_8 + \lambda_2\lambda_3\lambda_4\lambda_5 + \lambda_2\lambda_3\lambda_4\lambda_6 + \lambda_2\lambda_3\lambda_4\lambda_8 + \lambda_2\lambda_3\lambda_5\lambda_6 + \lambda_2\lambda_3\lambda_5\lambda_8 + \lambda_2\lambda_3\lambda_6\lambda_8 + \lambda_2\lambda_4\lambda_5\lambda_6 + \lambda_2\lambda_4\lambda_5\lambda_8 + \lambda_2\lambda_4\lambda_6\lambda_8 + \lambda_2\lambda_5\lambda_6\lambda_8 + \lambda_3\lambda_4\lambda_5\lambda_6 + \lambda_3\lambda_4\lambda_5\lambda_8 + \lambda_3\lambda_4\lambda_6\lambda_8 + \lambda_3\lambda_5\lambda_6\lambda_8 + \lambda_4\lambda_5\lambda_6 + \lambda_4\lambda_5\lambda_8\lambda_6 + \lambda_4\lambda_6\lambda_8) + p_1q_1\lambda_1\lambda_3(\lambda_2 + \lambda_4 + \lambda_6 + \lambda_8))$;
$f = (\lambda_1\lambda_2\lambda_3\lambda_4\lambda_5 + \lambda_1\lambda_2\lambda_3\lambda_4\lambda_6 + \lambda_1\lambda_2\lambda_3\lambda_4\lambda_8 + \lambda_1\lambda_2\lambda_3\lambda_5\lambda_6 + \lambda_1\lambda_2\lambda_3\lambda_5\lambda_8 + \lambda_1\lambda_2\lambda_3\lambda_6\lambda_8 + \lambda_1\lambda_2\lambda_4\lambda_5\lambda_6 + \lambda_1\lambda_2\lambda_4\lambda_5\lambda_8 + \lambda_1\lambda_2\lambda_4\lambda_6\lambda_8 + \lambda_1\lambda_2\lambda_5\lambda_6\lambda_8 + 2\lambda_1\lambda_3\lambda_4\lambda_5 + 2\lambda_1\lambda_3\lambda_4\lambda_6 + 2\lambda_1\lambda_3\lambda_4\lambda_8 + \lambda_1\lambda_3\lambda_4\lambda_5\lambda_6 + \lambda_1\lambda_3\lambda_4\lambda_5\lambda_8 + \lambda_1\lambda_3\lambda_4\lambda_6\lambda_8 + \lambda_1\lambda_3\lambda_5\lambda_8 + \lambda_1\lambda_3\lambda_6\lambda_8 + \lambda_1\lambda_4\lambda_5\lambda_6 + \lambda_1\lambda_4\lambda_5\lambda_8 + \lambda_1\lambda_4\lambda_6\lambda_8 + \lambda_1\lambda_5\lambda_6\lambda_8 + \lambda_2\lambda_3\lambda_4\lambda_5 + \lambda_2\lambda_3\lambda_4\lambda_6 + \lambda_2\lambda_3\lambda_4\lambda_8 + \lambda_2\lambda_3\lambda_5\lambda_6 + \lambda_2\lambda_3\lambda_5\lambda_8 + \lambda_2\lambda_3\lambda_6\lambda_8 + \lambda_2\lambda_4\lambda_5\lambda_6 + \lambda_2\lambda_4\lambda_5\lambda_8 + \lambda_2\lambda_4\lambda_6\lambda_8 + \lambda_2\lambda_5\lambda_6\lambda_8 + \lambda_3\lambda_4\lambda_5\lambda_6 + \lambda_3\lambda_4\lambda_5\lambda_8 + \lambda_3\lambda_4\lambda_6\lambda_8 + \lambda_3\lambda_5\lambda_6\lambda_8 + \lambda_4\lambda_5\lambda_6 + \lambda_4\lambda_5\lambda_8\lambda_6 + \lambda_4\lambda_8 - p_1q_1\lambda_1\lambda_3(\lambda_2\lambda_4 + \lambda_2\lambda_6 + \lambda_2\lambda_8 + \lambda_4\lambda_6 + \lambda_4\lambda_8 + \lambda_6\lambda_8))$;
$g = -((\lambda_1\lambda_2\lambda_3\lambda_4\lambda_5\lambda_6\lambda_8 + p_1q_1\lambda_1\lambda_3(\lambda_2\lambda_4\lambda_6\lambda_8) + p_1p_2p_3q_2q_3\lambda_1\lambda_2\lambda_4\lambda_6\lambda_8)$;
$h = -p_1p_2p_3q_2q_3\lambda_1\lambda_2\lambda_4\lambda_6\lambda_8\lambda_3$.

The conducted studies reveal that in GERT networks similar to Figure 2, there are no straightforward methods for identifying singular points of the function $\Phi_E(z)$ real variable substitution $(z = -i\varsigma)$, where ς is a real variable. This is because finding singular points involves solving nonlinear equations, and the complexity of the original equation increases with the complexity of the GERT network structure. Therefore, through complex transformations during modeling, we obtain the following expression:

$$\Phi(z) = \frac{(z^4 - yz^3 + uz^2 - xz + c)}{(\lambda_7 - s)(-1 \times (z^7 + vz^6 + bz^5 + az^4 + dz^3 + fz^2 + gz + h))} \tag{6}$$

The probability density distribution of the "interaction" time with the tracking object is:

$$\varphi(x) = \frac{1}{2\pi i}\int_{-i\infty}^{i\infty} e^{zx}\frac{(z^4 - yz^3 + uz^2 - xz + c)}{(-1 \times (z^7 + vz^6 + bz^5 + az^4 + dz^3 + fz^2 + gz + h))}dz, \tag{7}$$

where the integration is performed over the Bromwich contour [23].

The integration method is determined by the presence of simple poles or poles of some order in the function. If the function contains only simple poles, the expression can be written as follows:

$$e^{zx}\Phi(z) = \frac{e^{zx}(z^4 - yz^3 + uz^2 - xz + c)}{z^8 - w_7z^7 - w_6z^6 - w_5z^5 - w_4z^4 - w_3z^3 - w_2z^2 - w_1z + w_0} = \frac{\mu(z)}{\psi(z)}, \tag{8}$$

where $w_7 = (\lambda_7 - v)$;
$w_6 = (\lambda_7 v - b)$;

$w_5 = (\lambda_7 b - a)$;
$w_4 = (\lambda_7 a - d)$;
$w_3 = (\lambda_7 d - f)$;
$w_2 = (\lambda_7 f - g)$;
$w_1 = (\lambda_7 g - h)$;
$w_0 = (\lambda_7 h)$.

Thus, the distribution density of the "interaction" time with the tracking object is:

$$\varphi(x) = \sum_{k=1}^{8} \mathrm{Res}[e^{zx}\Phi(z)] = \sum_{k=1}^{8} \frac{\mu(z_k)}{\psi(z_k)} = \\ = \sum_{k=1}^{8} \frac{e^{zx}\left(z^4 - yz^3 + uz^2 - xz + c\right)}{8z^7 - 7w_7z^6 - 6w_6z^5 - 5w_5z^4 - 4w_4z^3 - 3w_3z^2 - 2w_2z - w_1} \quad (9)$$

The function may have not only simple poles, determined by the roots of the equation

$$z^8 - w_7z^7 - w_6z^6 - w_5z^5 - w_4z^4 - w_3z^3 - w_2z^2 - w_1z + w_0 = 0, \quad (10)$$

but also poles of higher order. This happens when λ_7 equals z. In such cases, the distribution density of the "interaction" time with the tracking object is calculated using the expression for finding residues at the poles of the corresponding order.

Thus, a mathematical model of radar operation under jamming conditions was developed based on the exponential GERT network. This model takes into account the main steps of the target trajectory tracking algorithm based on data from a single radar and provides a comprehensive approach to accounting for probabilistic and time characteristics, which distinguishes it from existing models.

This model can be used to study information processes in the systems where radars interact with tracking objects.

The use of exponential stochastic GERT models allows for the analytical treatment of results (e.g., functions and distribution densities) for comparative analysis and research. It also enables the study of complex, critical information and control systems using mathematical methods.

Despite the effectiveness of the GERT model for analyzing processes at the macro level, its capabilities in detailing local operations, such as precise target tracking under noise and interference conditions, are limited. To achieve higher accuracy at the trajectory level, methods capable of effectively accounting for the dynamic nature of systems and performing recursive state estimations are required. In this context, the Kalman filter serves as a suitable complement to the GERT model.

4. Modeling the Target Tracking Process Using Kalman Filters

Radar systems, especially under interference conditions, face challenges in accurately tracking targets. During the modeling of these systems, GERT models provide a powerful tool for analyzing complex probabilistic processes, such as multipath delays, interactions between states, and temporal dependencies. However, for precise target tracking, where local parameter estimation—such as position and velocity—is critical, GERT models have the following limitations:

- Macro-level nature of the GERT model: GERT networks excel at describing overall temporal and probabilistic characteristics of processes. However, they are not designed to estimate micro-level parameters, such as precise real-time target coordinates;
- Limitations in dynamic data processing: GERT models do not support the iterative refinement process necessary for real-time data processing. Under noisy and highly uncertain conditions, a method capable of adapting to changes is required;

- Error minimization challenge: For target tracking tasks, minimizing the root mean square error (RMSE) and ensuring robustness to false alarms are critical. GERT is not capable of effectively accounting for measurement noise and dynamic changes.

While GERT networks offer macro-level insights, they lack the precision required for real-time trajectory refinement, necessitating the use of complementary techniques like Kalman filtering.

In this regard, the use of Kalman filters becomes essential. They offer powerful capabilities for solving recursive filtering problems, accounting for noise, predicting target states, and refining estimates.

The GERT model provides a probabilistic and temporal foundation for analyzing general processes, while the Kalman filter complements it.

The Kalman filter is a powerful recursive algorithm used to estimate the state of a dynamic system under noisy and uncertain conditions. The operation of the filter involves two key stages:

- Prediction. This stage predicts the next state of the object based on its motion model.
- Correction. At this stage, the prediction is adjusted using the incoming measurements, minimizing errors and accounting for system noise.

The prediction stage is used to compute the future state of the object based on the current estimate and the dynamics model. At this stage, the state of the object (e.g., its position and velocity) is updated according to the equation:

$$\hat{x}_{k|k-1} = A_k \hat{x}_{k-1|k-1} + B_k u_k$$

where

$\hat{x}_{k|k-1}$ is the predicted state of the system at step k;

A_k is the state transition matrix, which describes the dynamics of the object;

$\hat{x}_{k-1|k-1}$ is the previous adjusted status;

$B_k u_k$ is the influence of the control action, where B_k is the control matrix and u_k is the vector of control parameters (if any).

Prediction of the error covariance: The state error covariance is updated to account for the process noise:

$$P_{k|k-1} = A_k P_{k-1|k-1} A_k^T + Q_k ,$$

where

$P_{k|k-1}$ is the error covariance matrix for the predicted state;

Q_k is the process noise covariance matrix (characterizes dynamic uncertainty of the system).

This stage provides a prediction of the future state of the object, which will subsequently be refined during the correction stage.

The correction stage is used to adjust the predicted state based on new measurement data. This allows the filter to account for observation errors and minimize deviations.

Calculation of the Kalman gain: The Kalman gain determines the extent to which the measurement data should influence the state update:

$$K_k = P_{k|k-1} H_k^T \left(H_k P_{k|k-1} H_k^T + R_k \right)^{-1},$$

where

H_k is the observation matrix (relates the state of the system to the measured quantities);

R_k is the measurement noise covariance matrix (describes the uncertainty of measurement data).

The predicted state is being refined in the light of new data:

$$\hat{x}_{k|k} = \hat{x}_{k|k-1} + K_k\left(z_k - H_k\hat{x}_{k|k-1}\right),$$

where

z_k is the vector of measurements at step k;

$z_k - H_k\hat{x}_{k|k-1}$ is the difference between measurements and the predicted state (observation error);

K_k is the Kalman gain.

The error covariance matrix is updated to reflect the reduced non-certainty:

$$P_{k|k} = (I - K_k\, H_k\,)P_{k|k-1}\,,$$

where

$P_{k|k}$ is the updated state covariance matrix;

I is the unit matrix.

These stages are implemented based on the state and measurement equations, where the transition matrices, process noise covariance, and measurement noise covariance play a key role. A more detailed description of the algorithm can be found, for example, in works [24–27], where the corresponding formulas and application examples are presented.

In the context of our study, the Kalman filter is used to refine the trajectories obtained after the initial data processing. During the prediction stage, the target motion model, including its maneuverability, is taken into account. The correction stage reduces the impact of noise arising during the measurement of target coordinates and velocities.

The use of the Kalman filter in combination with GERT models allows the integration of the advantages of both approaches, providing both macro-level process analysis and micro-level data detailing. This integration opens up opportunities for developing a flexible and accurate target tracking model in radar systems, especially under conditions of high uncertainty and noise.

The connection between the two approaches can be represented as a sequence of stages and operations. The GERT model enables the following operations:

- Models the high-level process of target detection and tracking;
- Describes probabilistic state transitions and time delays.

The Kalman filter takes data generated by the GERT model and uses it as initial conditions for its operation. After the first step, the Kalman filter refines the local target trajectories, minimizing the influence of noise.

This integration accounts for both macro-level and micro-level aspects of radar systems. At the macro level, the overall process structure is analyzed, including the impact of different states and probabilities. At the micro level, tracking accuracy is improved through detailed data processing.

The proposed approach offers several advantages:

- Improved accuracy. The Kalman filter reduces uncertainty caused by noise and interference, improving the quality of data provided by the GERT model;
- Robustness to interference. The GERT model accounts for complex probabilistic scenarios, while the Kalman filter adapts to changing real-time conditions;
- Efficiency. The combination of both approaches ensures a balanced workload: the GERT model manages the overall process structure, while the Kalman filter focuses on local tasks.

Figure 3 presents a structural diagram illustrating the relationship between the GERT model and the Kalman filter.

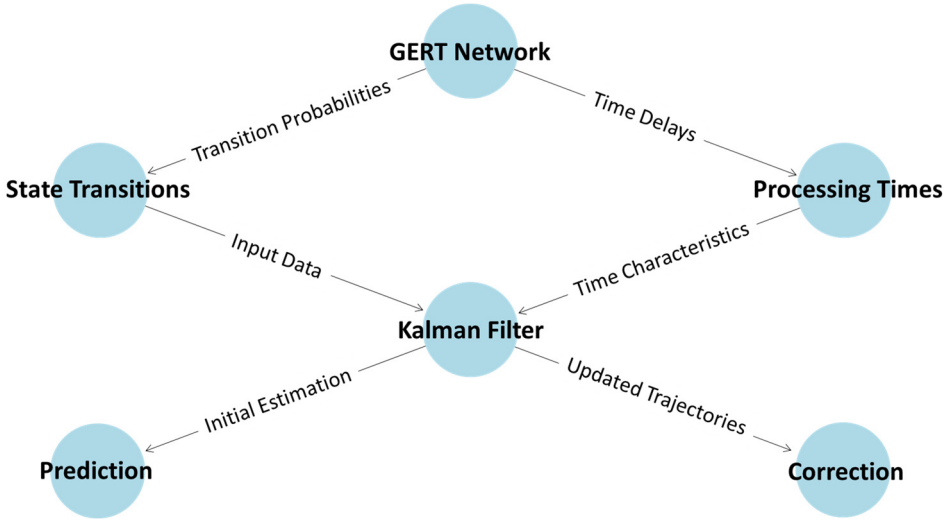

Figure 3. Structural diagram of the relationship between the GERT model and the Kalman filter.

As an example of implementing the mathematical model complex, the following algorithm is presented and implemented:

Step 1. Target Detection (GERT). The GERT model simulates the detection process and determines the probabilities and time characteristics of target detection.

Step 2. Initial State Estimation (GERT). The GERT model provides a probabilistic estimate of the target's position and its initial trajectory.

Step 3. Trajectory Refinement (Kalman Filter). The Kalman filter refines the trajectory based on the data provided by the GERT model, minimizing errors and ensuring continuous tracking.

The results of the implementation and evaluation of the interaction between the two modeling approaches are presented in Figure 4.

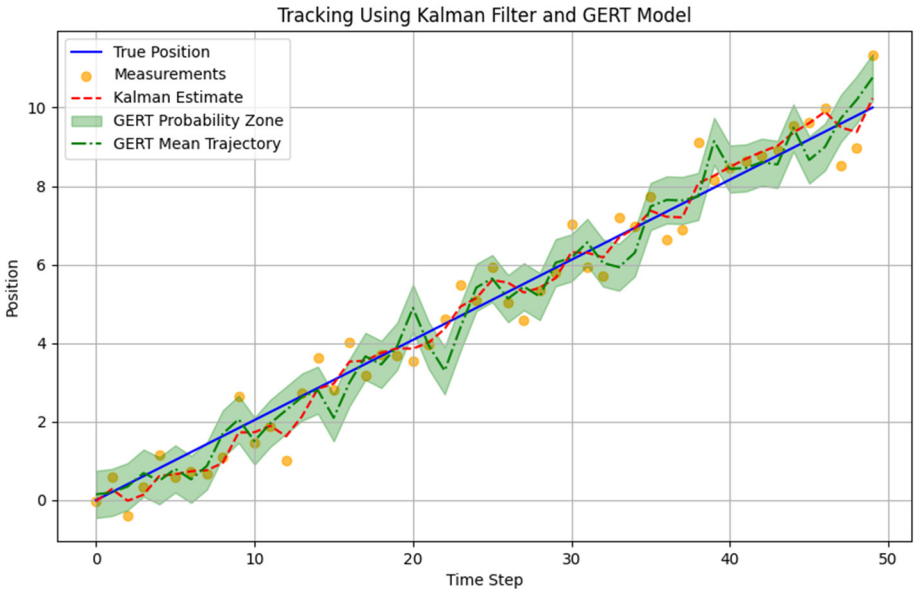

Figure 4. Comparison of trajectory predictions generated by the GERT model and Kalman filter, highlighting their complementary performance in interference conditions.

The simulation represented in Figure 4 is based on specific parameters and operational conditions that reflect real-world scenarios. The interference intensity (λ) ranges from 0.1, representing low external jamming, to 1, indicating high interference, which allows

the model to simulate various environmental conditions. The modeled target moves at a velocity of 200 m/s, characteristic of a maneuverable airborne object. The radar operates at a scan rate of 10 Hz, which is typical for medium-range detection systems and ensures frequent updates of tracking data.

To account for the effects of noise and variability, the noise covariance parameters (Q and R) are adjusted to reflect real-world sensor imperfections and process fluctuations. Additionally, the GERT network incorporates probabilistic states to model key radar processes, such as signal detection, trajectory establishment, and tracking. These states are interconnected through transitions that account for time delays and uncertainties introduced by interference conditions. This comprehensive parameter set enables a detailed analysis of radar system performance in challenging environments.

Figure 4 illustrates the process of object tracking using the Kalman filter and the GERT model, as well as their interaction for processing measurement data. The blue line represents the true position of the object at each time step, serving as a reference trajectory. This ideal position shows where the object is located at each moment in time without the influence of noise and uncertainty.

The orange points on the graph represent noisy measurements of the object's position, simulating data obtained from real sensors. These measurements deviate randomly from the true position due to noise, which is characteristic of any real observation system. Nevertheless, the measurements remain close enough to the true trajectory, allowing the Kalman filter to effectively use them for correcting the object's position.

The red dashed line demonstrates the object position estimates generated using the Kalman filter. This filter smooths the noisy measurements, minimizing deviations and bringing the estimates closer to the true trajectory. The results of the Kalman filter exhibit high accuracy, as its estimates closely match the reference trajectory.

The green dash-dotted line shows the mean trajectory predicted by the GERT model. This trajectory is based on probabilistic transitions and temporal characteristics determined by the GERT model. While it generally aligns with the true trajectory, the GERT predictions are less accurate due to their probabilistic nature. The green shaded area around the GERT mean line represents the model's uncertainty zone, showing the range of possible object positions. The expanded uncertainty zone highlights that the GERT model provides a broader, more generalized representation of the object's position, unlike the Kalman filter, which minimizes noise.

The combined use of the GERT model and the Kalman filter demonstrates their complementary nature. The GERT model accounts for the probabilistic characteristics of the system and provides an initial understanding of the possible range of object positions. The Kalman filter, in turn, refines the trajectory based on incoming measurement data, delivering precise estimates. This combined approach is particularly useful for tracking tasks where both high accuracy and consideration of system uncertainties are required. The graph clearly illustrates the differences between the approaches, their advantages, and their respective limitations.

5. Experiments and Results: Research of the Probability-Time Characteristics of the Interaction Channel Between the Radar and the Object That Puts Up Active Interference

Consider an example of radar–object interaction in the presence of active interference from the object.

Let us consider the following modeling parameters: interference intensity, λ, time intervals, T, and other input parameters of the model. Based on the analytical expression for the probability density function of the radar's interaction time with the target $p(t)$,

calculations were carried out for various values of interference intensity. The results are presented in the form of probability density function (PDF) and cumulative distribution function (CDF) graphs.

To model radar performance under interference conditions, parameters characteristic of modern radar systems were used. The interference intensity, λ, was chosen in the range of 0.1 to 1, corresponding to different scenarios, from weak natural interference to conditions of active electronic countermeasures. The radar's pulse repetition frequency (f) is 10 Hz, which is typical for medium-range detection and tracking systems. The target velocity (v) was set at 200 m/s, representing the parameters of highly maneuverable airborne objects. The radar's operational range (R) is 10 km, which is typical for ground-based short-range systems. These parameters allow the evaluation of the effectiveness of the proposed model in scenarios close to real-world operating conditions.

The modeling and calculations were performed using a Python 3.11-based simulation tool developed for this study. This software allows for the flexible implementation of radar parameters and interference conditions, as well as the dynamic visualization of results. The tool utilizes NumPy for numerical computations and Matplotlib for plotting graphs, ensuring precise and reliable results. Additionally, the interactive features of the software enable the real-time adjustment of key parameters such as λ, radar frequency (f), and target velocity (v) to evaluate their influence on radar performance.

Figure 5 shows the graph of the dependence of the radar's mean response time on different interference intensities.

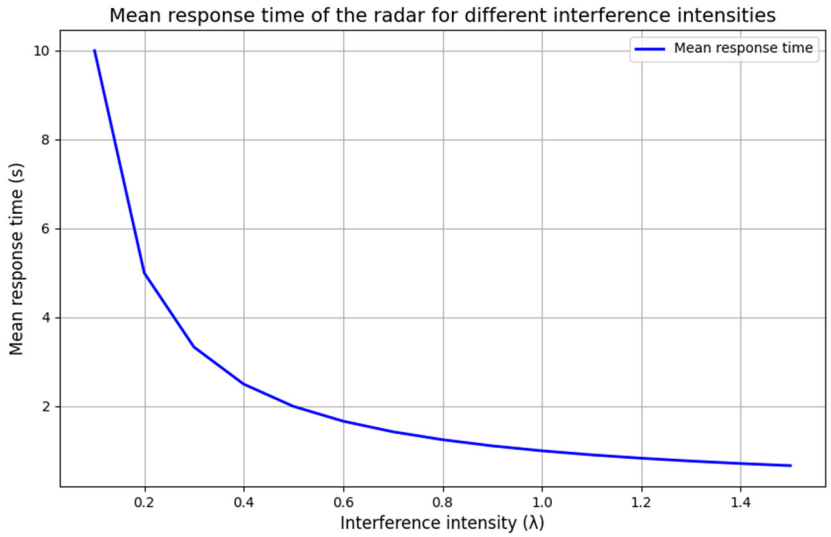

Figure 5. The graph of the dependence of the radar's mean response time on different interference intensities.

As seen from the graph, at low interference intensity ($\lambda \approx 0.1$), the mean response time reaches its maximum value ($t^{-} \approx 10$ s). With an increase in interference intensity ($\lambda > 1.00$), the mean response time decreases sharply and asymptotically approaches a value of approximately 1.5 s.

The mean response time is an important parameter that reflects the radar's performance dependence on interference levels. The reduction in response time with increasing λ is due to the fact that, under challenging conditions, the system is forced to complete data processing more quickly.

Figure 6 presents the probability graphs of interaction completion within specified time intervals. The graph demonstrates the radar's probability of completing interaction with a target within given time intervals (T = 10 s, 20 s, 30 s) at various values of λ. As can

be seen, for a short interval (T = 10 s), the probability of interaction completion increases rapidly with growing λ, reaching its maximum at $\lambda \approx 0.5$. For longer intervals (T = 20 s), the probability reaches 1 for nearly all values of λ, but at lower intensities ($\lambda \approx 0.1$), this growth occurs more slowly. The probability of interaction completion is higher for longer time intervals, as expected, since the radar has more time to complete its tasks.

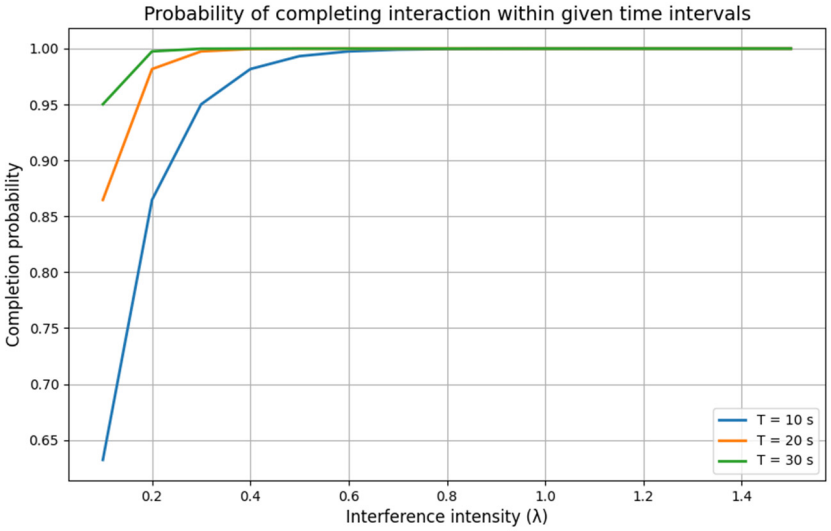

Figure 6. The probability graphs of interaction completion within specified time intervals.

These results demonstrate the influence of interference intensity and time constraints on radar performance and illustrate the applicability of the proposed model in analyzing radar operations under interference conditions.

Based on the algorithm in Figure 1, and following the analytical expressions (2–9) for calculating the equivalent W-function of radar operation, the distribution function, $\Phi(z)$, and the probability distribution density, $\varphi(x)$, of the "interaction" time with the tracking object, and also, using the features of the GERT model branches ($\lambda_1 > \lambda_2$, $\lambda_2 \approx \lambda_3 \approx \lambda_4 \approx \lambda_5, \lambda_6 \approx \lambda_7$) characteristic of this process, we study the probability-time characteristics (PTC) of the process.

Let us find the distribution density, $\varphi(x)$, probabilities of the message transmission time, provided that z are chosen as the roots of Equation (10) conditional probabilities and intensities in the GERT network branches have values: $p_1 = 0.9$, $q_1 = 0.4$, $p_2 = p_3 = 0.6$, $q_2 = q_3 = 0.4$, $\lambda_2 = 7$, $\lambda_3 = \lambda_4 = \lambda_5 = 6$, $\lambda_6 = \lambda_8 = 4$. Intensity, λ_1, takes the values:

(1) $\lambda_1 = 9$;
(2) $\lambda_1 = 5$;
(3) $\lambda_1 = 2$.

Taking into account the given GERT network features, along with in accordance the expression (9), we obtain:

$$\begin{aligned}\varphi(x) = \sum_{k=1}^{8} \operatorname{Res}[e^{zx}\Phi(z)] = \\ = \sum_{k=1}^{8} \frac{e^{(a+bi)x}\left((a+bi)^4 - y(a+bi)^3 + u(a+bi)^2 - x(a+bi) + c\right)}{8(a+bi)^7 - 7w_7z(a+bi)^6 - 6w_6(a+bi)^5 - 5w_5(a+bi)^4} \\ -4w_4(a+bi)^3 - 3w_3(a+bi)^2 - 2w_2(a+bi) - w_1 \\ - \frac{e^{(a+bi)x}\left((a-bi)^4 - y(a-bi)^3 + u(a-bi)^2 - x(a-bi) + c\right)}{8(a-bi)^7 - 7w_7z(a-bi)^6 - 6w_6(a-bi)^5 - 5w_5(a-bi)^4} \\ -4w_4(a-bi)^3 - 3w_3(a-bi)^2 - 2w_2(a-bi) - w_1\end{aligned} \quad (11)$$

Papers [22,23] show that the sum of the any fractional rational function values

$$f(z) = \frac{d_m z^m + d_{m-1} z^{m-1} + \ldots + d_1 z + d_0}{l_m z^m + l_{m-1} z^{m-1} + \ldots + l_1 z + l_0},\ d_m \neq 0,\ l_m \neq 0 \tag{12}$$

investigated for values of complex conjugate arguments can be represented in the form:

$$\frac{\tau + i\beta}{\gamma + i\beta} + \frac{\tau - i\delta}{\gamma - i\delta} \tag{13}$$

where $\tau, \beta, \gamma, \delta$ are some coefficients.

Using Euler's expressions [28]:

$$\begin{aligned} \varphi(x) = \sum_{k=1}^{8} \mathrm{Res}[e^{zx}\Phi(z)] = e^{(a+bi)x}\frac{\tau+i\beta}{\gamma+i\beta} + e^{(a+bi)x}\frac{\tau-i\delta}{\gamma-i\delta} = \\ = \frac{2e^{ax}}{\gamma^2+\delta^2}((\tau\gamma+\beta\delta)\cos(bx) + (\tau\gamma-\beta\delta)sin(bx)) \end{aligned} \tag{14}$$

The ensembles of the distribution function curves, $\Phi(x)$, and probability distribution density, $\varphi(x)$, for the radar "interaction" time with the tracking object are represented in Figures 7 and 8.

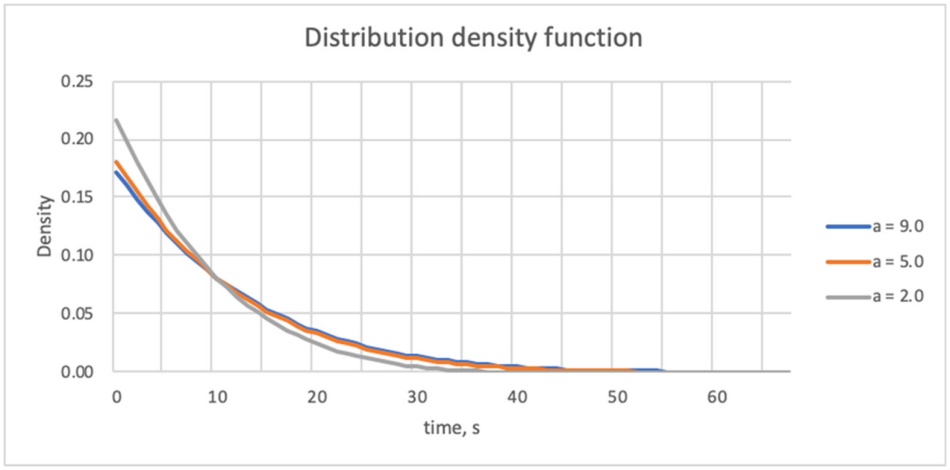

Figure 7. The probability distribution density $\varphi(x)$ graph of the radar "interaction" time with the tracking object.

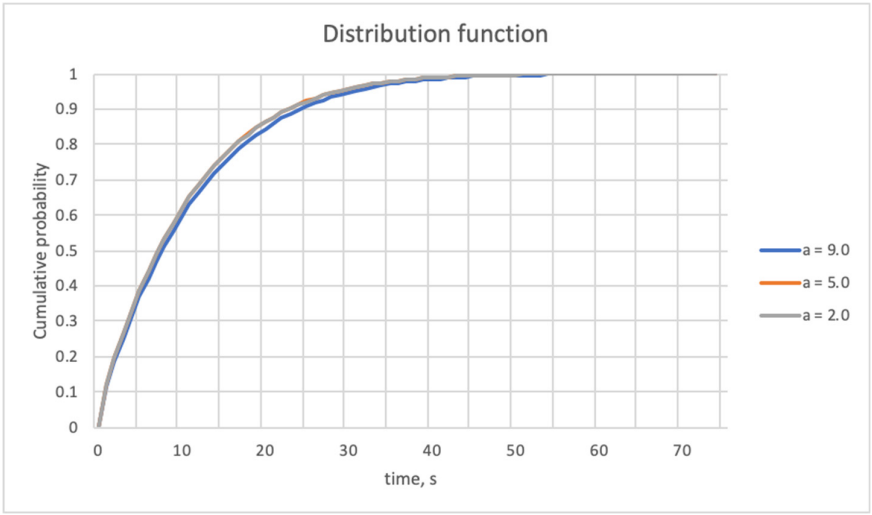

Figure 8. The distribution function, $\Phi(x)$, graphs of the radar "interaction" time with the tracking object.

Figure 7 illustrates the "rate" at which the probability values decrease for the radar system to complete interaction with the object within a specified time frame. The graph helps assess how much time the radar system will need to finish tracking the object under different interference scenarios.

At a high intensity of external influences ($\lambda = 9.0$), the probability of completing the interaction reaches its maximum within shorter time intervals. As the intensity of external influences decreases, the probability of completing the interaction also decreases. These results confirm the practical applicability of the model and its utility for studies at different interference intensity levels.

Similar results can be observed in Figure 8. This figure shows that at $\lambda = 9.0$, the probability density peak occurs within a shorter time span, indicating rapid completion of the interaction. At $\lambda = 5.0$, the peak occurs later, reflecting an increase in interaction time. At $\lambda = 2.0$, the probability is maximized over longer time intervals.

For the example presented above, the coefficients of the polynomial at $\lambda_1 = 9.0$:

$$[1.28835972e{+}06, -1.84190646e{+}06, 1.13882976e{+}06,$$

$$-3.97856880e{+}05, 8.59725600e{+}04, -1.17760000e{+}04,$$

$$9.99000000e{+}02, -4.80000000e{+}01, 1.00000000e{+}00]$$

The coefficients of the polynomial at $\lambda_1 = 5.0$:

$$[7.15755398e{+}05, -1.08779337e{+}06, 7.17163200e{+}05,$$

$$-2.68071600e{+}05, 6.22052000e{+}04, -9.18400000e{+}03,$$

$$8.43000000e{+}02, -4.40000000e{+}01, 1.00000000e{+}00]$$

The coefficients of the polynomial at $\lambda_1 = 2.0$:

$$[2.86302159e{+}05, -5.22208547e{+}05, 4.00913280e{+}05,$$

$$-1.70732640e{+}05, 4.43796800e{+}04, -7.24000000e{+}03,$$

$$7.26000000e{+}02, -4.10000000e{+}01, 1.00000000e{+}00]$$

Let us evaluate the reliability of the results obtained as a result of mathematical modeling. To check this hypothesis about the compliance of the results will use reliability criteria according to the Pearson χ^2 criterion [29–31]:

$$\chi^2 = N^* \sum_{i=1}^{k} \frac{(P_i^* - P_i)^2}{P_i}, \tag{15}$$

where k is the number of digits (intervals) of the statistical series;

P_i^* and P_i are the "statistical" and theoretical probabilities of the event.

As a result of the experiment, theoretical values, χ^2, and a tabular value, $\overline{\chi^2}$, were obtained as the inverse of the right-hand probability distribution, χ^2.

The conducted verification showed that the proposed hypothesis can be considered plausible or, at least, does not contradict the results obtained in mathematical modeling. This is confirmed by the fact that with a sufficiently large value of the confidence probability $Q = 0.95$ for all considered $\lambda_1 (\lambda_1 = 9; \lambda_1 = 5; \lambda_1 = 2)$, the corresponding values χ^2 ($\chi_1^2 = 19.1$, $\chi_2^2 = 14.5$, $\chi_3^2 = 12.2$) are much less than $\overline{\chi^2} = 99.1$, which allows us to recognize the discrepancies between the "statistical" (P_i^*) and theoretical (P_i) probabilities of the event occurrence as insignificant.

The accuracy of the developed model can be evaluated through a comparative study with mathematical models using similar formalization approaches. One such approach is mathematical modeling with Markov networks. However, it should be noted that GERT networks can more precisely model complex systems with multiple dependencies and probabilistic scenarios. In contrast, the advantage of Markov networks lies in their higher accuracy for tasks with fewer complex dependencies when strictly defined.

For the comparative study, the models described in [24,25] were chosen as prototypes. Among the possible comparison metrics, the authors selected the Kullback–Leibler divergence (KL-divergence) and the Wasserstein distance. Both metrics are widely used in statistical analysis and information theory, making them reliable tools for distribution analysis.

Figures 9 and 10 present the comparison results as curves of the cumulative distribution function (CDF) and probability density function (PDF) of the radar system's "interaction" time with the tracking object, respectively.

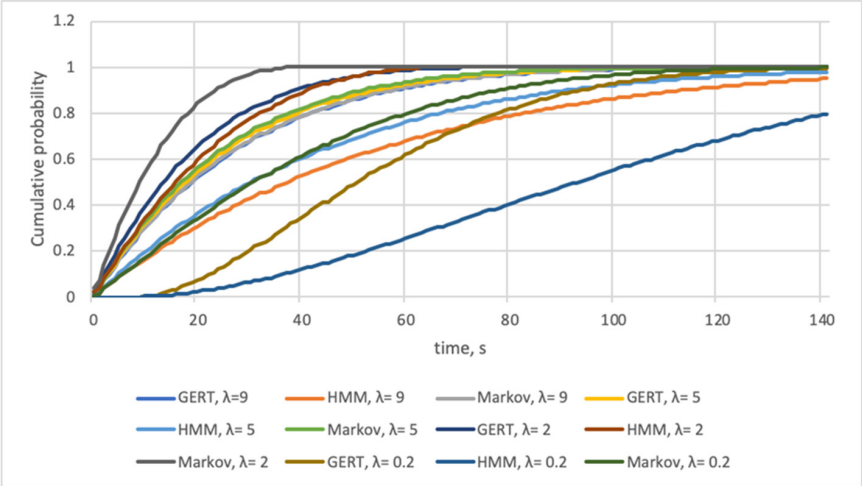

Figure 9. The cumulative distribution function (CDF) graphs of the radar system's "interaction" time with the tracking object for different modeling technologies (GERT, Markov networks, Hidden Markov Model).

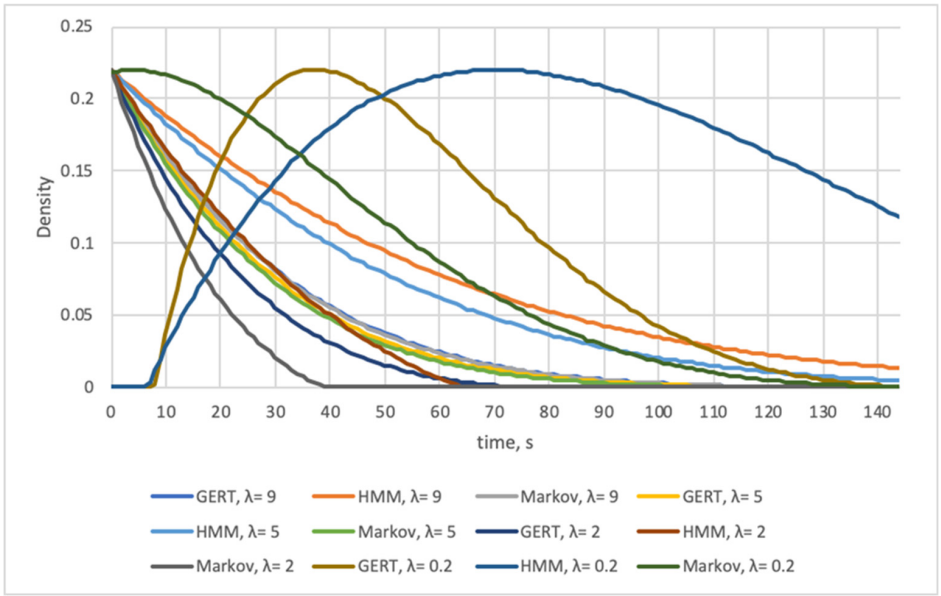

Figure 10. The probability density function (PDF) graphs for the radar system's "interaction" time with the tracking object (GERT, Markov networks, Hidden Markov Models).

Figures 9 and 10 illustrate that the GERT model demonstrates a more gradual change in cumulative probability, which is due to the probabilistic structure of network processes and their multiple pathways—characteristic of GERT modeling. Meanwhile, the hidden Markov model (HMM) and Markov models show a sharper accumulation of probability, reflecting their more straightforward probabilistic trajectories.

Additionally, the GERT results appear smoother and less abrupt compared to HMM. Further research is needed to gain a deeper understanding of the reasons for these differences.

Table 2 presents a comparison of the developed GERT model with prototype models [24–27], evaluated through KL-divergence and Wasserstein distance, highlighting the probabilistic and temporal accuracies of each model under varying interference intensities.

Table 2. Comparison results of the developed GERT model and prototype models.

Models—Research Prototypes	Research Parameters	GERT-Model			
		λ = 9	λ = 5	λ = 2	λ = 0.2
Markov model	KL-divergence	0.0001	0.0013	1.7714	0.2945
	Wasserstein distance	0.0016	0.0066	0.1451	0.0217
Hidden Markov Model	KL-divergence	0.2147	0.1413	0.0909	0.4969
	Wasserstein distance	0.1037	0.0832	0.1909	0.1346

As part of this study, a comparison of the GERT, Kalman filter, Markov, and HMM approaches was conducted to analyze radar systems under jamming conditions. The primary focus was on their individual advantages. GERT enables the modeling of temporal and probabilistic dependencies at the macro level, providing an overall structure for processes. At the same time, the Kalman filter ensures high accuracy at the micro level, minimizing the impact of noise when refining trajectories.

Comparative metrics such as KL-divergence and Wasserstein distance were used for quantitative analysis, highlighting differences in probability distributions between the models. These results emphasize the unique features and application areas of each model.

Based on the comparison results between the GERT model, the Markov model, and the HMM, several conclusions can be drawn regarding their characteristics and differences:

- At $\lambda = 9$, the KL-divergence for the Markov model is 0.0001, indicating a high similarity with the GERT model. This is also observed for other λ values, except for $\lambda = 0.2$, where a significant increase in KL-divergence is observed as the intensity decreases;
- The KL-divergence for HMM is significantly higher, indicating a greater discrepancy between GERT and HMM. This suggests that HMM is better suited for describing more complex dynamics but may not always align with GERT, especially at lower λ values;
- Low values of the Wasserstein distance between GERT and the Markov model (e.g., 0.0016 at $\lambda = 9$ and 0.0066 at $\lambda = 5$) indicate a close match in distributions, consistent with the low KL-divergence;
- The Wasserstein distance between GERT and HMM is also noticeable (e.g., 0.1037 at $\lambda = 9$ and 0.0832 at $\lambda = 5$), confirming that HMM differs more from GERT than the Markov model;
- As the intensity value, λ, decreases, both the KL-divergence and Wasserstein distance increase for all models. This may indicate that as λ decreases, the models become less similar, possibly due to changes in the structure of the data they are modeling;

- At $\lambda = 0.2$, the highest values for KL-divergence and Wasserstein distance are observed, suggesting greater complexity and diversity in the data.

6. Discussion

Preliminary analysis of the results suggests that further research in radar operation under jamming conditions is both relevant and feasible. Potential research directions include the following:

1. Improved Adaptive Algorithms. Developing more adaptive algorithms for tracking target trajectories under complex jamming conditions, potentially incorporating deep learning and neural network approaches for greater resilience to dynamic environmental changes;
2. New Jamming Models. Formalizing and modeling more complex jamming scenarios, such as disinformation attacks and electronic interference, to better assess external factors' effects on radar systems;
3. Comparative Analysis of Algorithms. Conducting comparative analyses of tracking algorithms to evaluate their effectiveness under various conditions, including testing on real or simulated data;
4. Technology Integration. Exploring the integration of technologies such as active electronically scanned array systems and advanced signal processing techniques for more efficient radar systems;
5. Weather Impact Assessment. Studying the impact of weather conditions on radar operation, with the goal of developing methods to mitigate their effects;
6. Cross-Disciplinary Research. Combining approaches from telecommunications, control systems, and informatics to create adaptable solutions for radar systems and other technologies operating under uncertainty.

The article presents results comparing models with a similar approach to mathematical formalization. It is important to note that these models (Kalman filters, Hidden Markov Models, Bayesian networks, etc.) [2–6,24–27] are applied in conditions of uncertainty and interference; however, each has its limitations, especially in complex multilayered systems. For instance, Kalman filters perform well in handling noise in linear systems, but their effectiveness can diminish in complex nonlinear scenarios with high interference density. Similarly, the HMM modeling approach assumes the existence of hidden states and requires significant computational resources for accurate modeling. GERT networks may offer greater flexibility, particularly in interference conditions where not only state probabilities but also the temporal structure of signals is important.

It is worth acknowledging that the proposed model largely relies on theoretical assumptions. One limitation may be the necessity of using a larger volume of experimental data to validate the proposed model in real-world conditions. There is also a significant potential issue regarding the scalability of the model to more complex systems with a high level of interference. Furthermore, the article generalizes the concept of "factors affecting the efficiency of radar systems". This is a rather vague formulation that can be misleading. In the future, it is essential to focus on specific examples of interference that impact the system's performance with clear justification.

7. Conclusions

This study developed a mathematical model for radar operation, allowing visualization and formalization of complex processes, including probabilistic dependencies and time characteristics, particularly at the initial stages of target acquisition and tracking. The model's key feature is its integrated approach to accounting for these characteris-

tics. Analytical assessments of the system's probabilistic, time, and spatial characteristics were obtained.

Additionally, as part of this study, a Kalman filter-based model was developed and integrated to refine the trajectories predicted by the GERT model. The Kalman filter ensures precise smoothing of noisy measurements and minimizes deviations from the true trajectory of the object. This enables the GERT model to serve as a tool for primary probabilistic analysis, while the Kalman filter performs the functions of trajectory refinement and improving prediction accuracy. Such a combined use of models provides a more comprehensive description and understanding of the dynamics of radar system interactions with objects.

The analysis of the Kalman filter demonstrated its high efficiency in conditions of significant noise and uncertainty. At the same time, the GERT model continues to play an important role in accounting for the temporal and probabilistic characteristics of the system, as well as in forming the initial conditions for further data refinement. The combined use of the GERT model and the Kalman filter allows for both the probabilistic nature of the system to be considered and measurement errors to be minimized, which is particularly critical for tracking systems operating in interference-heavy environments.

The study of the target trajectory tracking algorithm's block diagram based on data from a single radar suggests that prioritizing performance indicators is crucial. The choice of probabilistic and time indicators led to the formulation of the concept of GERT–network modeling for radar–object interaction. A mathematical model of radar operation under interference conditions was then developed, yielding distribution function curves, $\Phi(x)$, and probability distribution density, $\varphi(x)$, along with polynomial coefficients for different generating function intensities.

The comparative study with prototype models illustrated that models based on Markov network technologies align reasonably well with the GERT model, particularly at high values of the parameter λ. However, as λ decreases, there is an increase in both KL-divergence and Wasserstein distance, indicating limited accuracy under these conditions. Thus, the proposed GERT model proves to be more accurate and effective.

The comparison with HMM revealed that while this model can account for hidden states, its complexity may lead to discrepancies with the GERT model, especially under low λ conditions.

The model can be utilized to enhance the efficiency of collision warning systems, object tracking, and improve tracking systems' performance in high interference environments. In the future, it may be possible to expand the model using fuzzy GERT networks and neural networks, making it more adaptive to changing operational conditions.

Author Contributions: Supervision and conceptualization: S.S. and V.D.; methodology: S.S.; experiments, result visualization, and analysis: M.K.-K., P.M., Y.T., V.V., O.V. and V.B.; verification of theoretical and experimental conclusions: S.S.; writing—original draft: V.D. and S.S. All authors have read and agreed to the published version of the manuscript.

Funding: This research received no external funding.

Institutional Review Board Statement: Not applicable.

Informed Consent Statement: Not applicable.

Data Availability Statement: The raw data supporting the conclusions of this article will be made available by the authors on request.

Acknowledgments: The authors appreciate the scientific society of the consortium and, in particular, the staff of the Department of Computer Systems, Networks and Cybersecurity (DCSNCS) at the Cyber Security Department, University of the National Education Commission (Krakow, Poland), Department of Information Systems, National Technical University "Kharkiv Polytechnic Institute",

Kyrpychova str., 2, Kharkiv, Ukraine, Science Entrepreneurship Technology University M. Shpaka st., 3, Kiyv, Ukraine and for invaluable inspiration and creative analysis during the preparation of this paper.

Conflicts of Interest: The authors declare no conflicts of interest.

References

1. Skolnik, M.I. *Introduction to Radar Systems*, 3rd ed.; McGraw Hill Higher Education International Publisher: New York, NY, USA, 2002; ISBN-13: 9780072881387/9780071181891/9780072909807.
2. Griffiths, H.; Cohen, L.; Watts, S.; Mokole, E.; Baker, C.; Wicks, M.; Blunt, S. Radar Spectrum Engineering and Management: Technical and Regulatory Issues. *Proc. IEEE* **2015**, *103*, 85–102. [CrossRef]
3. Gini, F.; Farina, A. Vector subspace detection in compound-Gaussian clutter. Part I: Survey and new results. *IEEE Trans. Aerosp. Electron. Syst.* **2002**, *38*, 1295–1311. [CrossRef]
4. Tian, F.; Guo, X.; Fu, W. Target Tracking Algorithm Based on Adaptive Strong Tracking Extended Kalman Filter. *Electronics* **2024**, *13*, 652. [CrossRef]
5. Sun, Y.-C.; Kim, D.; Hwang, I. Multiple-model Gaussian mixture probability hypothesis density filter based on jump Markov system with state-dependent probabilities. *IET Radar Sonar Navig.* **2022**, *16*, 1881–1894. [CrossRef]
6. Alsheikhy, A.; Almutiry, M. Performance Evaluation in a Radar System. *IJCSNS Int. J. Comput. Sci. Netw. Secur.* **2018**, *18*, 116.
7. Chen, D.; Shi, S.; Gu, X.; Shim, B. Robust DoA Estimation Using Denoising Autoencoder and Deep Neural Networks. *IEEE Access* **2022**, *10*, 52551–52564. [CrossRef]
8. Semenov, S.; Kolisnyk, T.; Oksana, S.; Roh, V. Intelligent extraction of the informative features for UAV motion modelling: Principles and techniques. In Proceedings of the 2023 13th International Conference on Dependable Systems, Services and Technologies (DESSERT), Athens, Greece, 13–15 October 2023; pp. 1–6.
9. Kozlovskyi, V.; Shvets, I.; Lysetskyi, Y.; Karpinski, M.; Shaikhanova, A.; Shangytbayeva, G. Control of Telecommunication Network Parameters under Conditions of Uncertainty of the Impact of Destabilizing Factors. *Information* **2024**, *15*, 69. [CrossRef]
10. Arroyo Cebeira, A.; Asensio Vicente, M. Adaptive IMM-UKF for Airborne Tracking. *Aerospace* **2023**, *10*, 698. [CrossRef]
11. Luo, M.; Sun, H.; Wu, W.; Xie, X.; Jiang, S. Improved multi-target tracking algorithm based on SMC-CBMeMBer for the airborne Doppler radar. *J. Eng.* **2019**, *2019*, 6377–6381. [CrossRef]
12. Semenov, S.; Zhang, L.; Cao, W.; Bulba, S.; Babenko, V.; Davydov, V. Development of a fuzzy GERT-model for investigating common software vulnerabilities. *East.-Eur. J. Enterp. Technol.* **2021**, *6*, 6–18. [CrossRef]
13. Semenov, S.; Liqiang, Z.; Weiling, C.; Davydov, V. Development a mathematical model for the software security testing first stage. *East.-Eur. J. Enterp. Technol.* **2021**, *3*, 24–34. [CrossRef]
14. Semenov, S.; Liqiang, Z.; Weiling, C. Penetration Testing Process Mathematical Model. In Proceedings of the 2020 IEEE International Conference on Problems of Infocommunications. Science and Technology (PIC S&T), Kharkiv, Ukraine, 6–9 October 2020; pp. 142–146. [CrossRef]
15. Kannanthara, J.; Griffiths, D.; Jahangir, M.; Jones, J.M.; Baker, C.J.; Antoniou, M.; Bell, C.J.; White, H.; Bongs, K.; Singh, Y. Whole system radar modelling: Simulation and validation. *IET Radar Sonar Navig.* **2023**, *17*, 1050–1060. [CrossRef]
16. Park, S.R.; Nam, I.; Noh, S. Modeling and Simulation for the Investigation of Radar Responses to Electronic Attacks in Electronic Warfare Environments. *Secur. Commun. Netw.* **2018**, *2018*, 3580536. [CrossRef]
17. Liu, X.; Li, D. Analysis of cooperative jamming against pulse compression radar based on CFAR. *EURASIP J. Adv. Signal Process.* **2018**, *2018*, 69. [CrossRef]
18. Niu, Z.; Chen, H.L.; Wang, X.Q.; Du, J.; Chen, S.Y.; Bi, Z.Y. Research on Radar Anti-jamming Performance Evaluation System in Complex Electromagnetic Environment. In Proceedings of the 2022 10th China Conference on Command and Control (C2 2022), Beijing, China, 7–9 July 2022; Lecture Notes in Electrical Engineering; Springer: Singapore, 2022; p. 949. [CrossRef]
19. Chen, Z.; Tang, J.; Zhang, X.Y.; So, D.K.C.; Jin, S.; Wong, K.-K. Hybrid Evolutionary-Based Sparse Channel Estimation for IRS-Assisted mmWave MIMO Systems. *IEEE Trans. Wirel. Commun.* **2022**, *21*, 1586–1601. [CrossRef]
20. Nandan, S.; Rahiman, M.A. Roadside Intelligence: Efficient Channel Estimation for IRS-Aided mmWave Vehicular Communication. *IEEE Access* **2024**, *12*, 115883–115894. [CrossRef]
21. Chen, J.; Wang, F.; Zhou, J. Information-Theoretic Optimal Radar Waveform Selection With Multi-Sensor Cooperation for LPI Purpose. *IEEE Access* **2022**, *10*, 113649–113661. [CrossRef]
22. El-Faheem, A.; Mustafa, A.; El-Hafeez, T. Improving the Reliability Performance for Radar System Based on Rayleigh Distribution. *Sci. Afr.* **2022**, *17*, e01290. [CrossRef]
23. Kluitenberg, G.; Knight, J.; Kamai, T. Integral form of the cylindrical perfect conductors solution for the dual-probe heat-pulse method. *Soil Sci. Soc. Am. J.* **2021**, *85*, 1963–1969. [CrossRef]

24. Kumar, T. Duraiswamy, Punithavathi. Optimization of Kalman Filter for Target Tracking Applications. In *Advances in Multidisciplinary Analysis and Optimization*; Springer: Berlin/Heidelberg, Germany, 2020. [CrossRef]
25. Aditya, P.; Apriliani, E.; Arif, D.; Baihaqi, K. Estimation of three-dimensional radar tracking using modified extended kalman filter. *J. Phys. Conf. Ser.* **2018**, *974*, 012071. [CrossRef]
26. Tugac, S.; Efe, M. Radar target detection using hidden Markov models. *Prog. Electromagn. Res. B* **2012**, *44*, 241–259. [CrossRef]
27. Haddad, B.; Adane, A.; Mesnard, F.; Sauvageot, H. Modeling anomalous radar propagation using first-order two-state Markov chains. *Atmos. Res.* **2000**, *52*, 283–292. [CrossRef]
28. Hernández, J.; Peralta, D.; Quintana, Y. A Look at Generalized Degenerate Bernoulli and Euler Matrices. *Mathematics* **2023**, *11*, 2731. [CrossRef]
29. Nihan, S. Karl Pearsons chi-square tests. *Educ. Res. Rev.* **2020**, *15*, 575–580. [CrossRef]
30. Crack, T.F. A Note on Karl Pearson's 1900 Chi-Squared Test: Two Derivations of the Asymptotic Distribution, and Uses in Goodness of Fit and Contingency Tests of Independence, and a Comparison with the Exact Sample Variance Chi-Square Result (November 14, 2018). Available online: https://papers.ssrn.com/sol3/papers.cfm?abstract_id=3284255 (accessed on 19 December 2024).
31. Kovalchuk, O.; Karpinski, M.; Babala, L.; Kasianchuk, M.; Shevchuk, R. The Canonical Discriminant Model of the Environmental Security Threats. *Complexity* **2023**, *2023*, 5584750. [CrossRef]